Zhang, Huina; Zhang, Yanli; Huang, Zhonghui; Acton, W. Joe F.; Wang, Zhaoyi; Nemitz, Eiko; Langford, Ben; Mullinger, Neil; Davison, Brian; Shi, Zongbo; Liu, Di; Song, Wei; Yang, Weiqiang; Zeng, Jianqiang; Wu, Zhenfeng; Fu, Pingqing; Zhang, Qiang; Wang, Xinming. 2020. **Vertical profiles of biogenic volatile organic compounds as observed online at a tower in Beijing.**

The definitive version was published in *Journal of Environmental Sciences*, 95. 33-42. 10.1016/j.jes.2020.03.032

Vertical profiles of biogenic volatile organic compounds as observed online at a tower in Beijing

Huina Zhang[1,3], Yanli Zhang[1,2,*], Zhonghui Huang[1,4], W. Joe F. Acton[5], Zhaoyi Wang[1], Eiko Nemitz[6], Ben Langford[6], Neil Mullinger[6], Brian Davison[5], Zongbo Shi[7,8], Di Liu[7], Wei Song[1], Weiqiang Yang[1], Jianqiang Zeng[1,2], Zhenfeng Wu[1,3], Pingqing Fu[8,9], Qiang Zhang[10], Xinming Wang[1,2,3]

1. State Key Laboratory of Organic Geochemistry and Guangdong Key Laboratory of Environmental Protection and Resources Utilization, Guangzhou Institute of Geochemistry, Chinese Academy of Sciences, Guangzhou 510640, China

2. Center for Excellence in Regional Atmospheric Environment Institute of Urban Environment, Chinese Academy of Sciences, Xiamen 361021, China

3. University of Chinese Academy of Sciences, Beijing 100049, China

4. State Environmental Protection Key Laboratory of Environmental Pollution Health Risk Assessment and Guangdong Key Laboratory of Water and Air Pollution Control, South China Institute of Environmental Science, Ministry of Ecology and Environment, Guangzhou 510655, China

5. Lancaster Environment Centre, Lancaster University, Lancaster LA14YQ, UK

6. Centre for Ecology and Hydrology, Edinburgh, EH26 0QB, UK

7. School of Geography Earth and Environmental Sciences, University of Birmingham, Birmingham B15 2TT, UK

8. Institute of Surface-Earth System Science, Tianjin University, Tianjin 300072, China

9. Institute of Atmospheric Physics, Chinese Academy of Sciences, Beijing 100029, China

10. Beijing Key Laboratory of Green Chemical Reaction Engineering and Technology, Department of Chemical Engineering, Tsinghua University, Beijing 100084, China

Abstract

Vertical profiles of isoprene and monoterpenes were measured by a proton transfer reaction-time of flight-mass spectrometry (PTR-ToF-MS) at heights of 3, 15, 32, 64, and 102 m above the ground on the Institute of Atmospheric Physics (IAP) tower in central Beijing during the winter of 2016 and the summer of 2017. Isoprene mixing ratios were larger in summer due to much stronger local emissions whereas monoterpenes were lower in summer due largely to their consumption by much higher levels of ozone. Isoprene mixing ratios were the highest at the 32 m in summer (1.64 ± 0.66 ppbV) and at 15 m in winter (1.41 ± 0.64 ppbV) with decreasing concentrations to the ground and to the 102 m, indicating emission from the tree canopy of the surrounding parks. Monoterpene mixing ratios were the highest at the 3 m height in both the winter (0.71 ± 0.42 ppbV) and summer (0.16 ± 0.10 ppbV) with a gradual decreasing trend to 102 m, indicting an emission from near the ground level. The lowest isoprene and monoterpene mixing ratios all occurred at 102 m, which were 0.71 ± 0.42 ppbV (winter) and 1.35 ± 0.51 ppbV (summer) for isoprene, and 0.42 ± 0.22 ppbV (winter) and 0.07 ± 0.06 ppbV (summer) for monoterpenes. Isoprene in the summer and monoterpenes in the winter, as observed at the five heights, showed significant mutual correlations. In the winter monoterpenes were positively correlated with combustion tracers CO and acetonitrile at 3 m, suggesting possible anthropogenic sources.

Keywords:

Isoprene

Monoterpenes

Vertical profiles

Proton transfer reaction-time of flight-mass spectrometry (PTR-ToF-MS)

Biogenic volatile organic compounds (BVOCs)

---

55 *Corresponding author. E-mail: zhang_yl86@gig.ac.cn (Yanli Zhang)
56

Introduction

Volatile organic compounds (VOCs) from both anthropogenic and biogenic sources play crucial roles in the formation of ozone (O_3) and secondary organic aerosols (SOA) in the atmosphere (Henze et al., 2006). Biogenic VOCs (BVOCs) are mainly emitted from plant leaves and they account for ~90% of global annual VOC emissions (Guenther et al., 2012). Due to their relatively higher reactivity with atmospheric oxidants (Ryerson et al., 2001; Hallquist et al., 2009), BVOCs like isoprene have exceedingly strong ozone formation potential (OFP) compared with many anthropogenic VOCs (Atkinson, 2000; Calfapietra et al., 2013). In addition, on a global scale, it is estimated that SOA derived from biogenic sources greatly exceed that from anthropogenic sources (Hallquist et al., 2009).

As BVOCs, such as isoprene (C_5H_8) and monoterpenes ($C_{10}H_{16}$), are largely emitted from vegetation, the majority of field observations have been carried out in natural ecosystems (Baker et al., 2005; Eerdekens et al., 2009; Bai et al., 2017). However, model results suggest that BVOCs could contribute as much as 15% of ground level O_3 pollution formed in some of the metropolitan areas of Europe (Curci et al., 2009). Recent studies have also showed that anthropogenic pollutants including SO_2 and oxides of nitrogen (NO_x, NO + NO_2) can largely promote SOA formation from BVOCs (Shilling et al., 2013; Xu et al., 2015). Monoterpenes are estimated to be the largest source of summer organic aerosol in the southeastern United States (Zhang et al., 2018), and BVOC-derived SOA tracers have been widely observed to occur in atmospheric aerosols over cities (Fu et al., 2009; Ding et al., 2012; Lin et al., 2013; Martinsson et al., 2017). Thus, the effect of BVOCs in the urban environment is an important but currently understudied area of research.

Measurements of the vertical distribution of pollutants offer insight into their

sources, and enable the evaluation of chemical transport models and assessing indoor pollution at different heights (Jo and Kim, 2002; Caputi et al., 2019). Aircrafts, tethered balloons and towers are the most common platforms used to assess vertical gradients of pollutants. Yet, aircrafts are typically limited to higher altitude measurements (> 200 m) (Reeves et al., 2010; He et al., 2012), and tethered balloons are typically confined to rural areas due to space requirements (Greenberg et al., 1999; Sun et al., 2018). Tower-based measurements are, therefore, the most suitable option for use in the urban environment (Hollaway et al., 2019). While, many previous tower-based studies have been conducted in forests (Hemig et al., 1998; Kesselmeier et al., 2002; Yanez-Serrano et al., 2015), we believe the results presented here represent some of the first vertical profiles of BVOCs measured above a major urban conurbation.

Like many cities in developing countries, Beijing has air quality problems including very high levels of O_3 and fine particulate matter. Numerous field campaigns have been conducted to characterize anthropogenic VOCs in Beijing (Liu et al., 2017; Yang et al., 2018), but relatively few studies have focused on the measurement of biogenic compounds such as isoprene and monoterpenes and those that have typically been confined to offline analytical techniques (Duan et al., 2008; Cheng et al., 2018; Mo et al., 2018). Since monoterpenes are highly reactive with O_3, inefficient removal of O_3 during sampling could lead to the loss of monoterpenes and an underestimation of their abundance (Fick et al., 2001; Arnts et al., 2008). Furthermore, wall adsorption and storage time may also influence the determination of BVOCs in bags and canisters samples (Ahn et al., 2016). In contrast, online instruments such as proton transfer reaction-time of flight-mass spectrometry (PTR-ToF-MS) overcome these shortcomings by offering real-time monitoring with a sample resolution on the order of seconds (de Gouw and Warneke, 2007; Liu et al., 2016; Huang et al., 2017; Yuan et al.,

2017).

In this study, mixing ratios of isoprene and monoterpenes were measured by a PTR-ToF-MS in the winter of 2016 and the summer of 2017 at 5 different heights from the 325-meter the Institute of Atmospheric Physics (IAP) tower in central Beijing. The aims of this study were (i) to obtain vertical profiles of isoprene and monoterpenes in urban Beijing, (ii) to explore the factors influencing their abundance, and (iii) to evaluate if these predominantly biogenic species also have a significant contribution from anthropogenic sources within Beijing.

1. Material and methods

1.1 Vertical Profile Measurements

Field measurements were conducted as part of the joint UK-China Atmospheric Pollution and Human Health in a Developing Megacity (APHH-Beijing) research programme. The monitoring site (39°58′33″ N, 116°22′41″ E) is located in the Institute of Atmospheric Physics, Chinese Academy of Sciences (IAP, CAS), which is an urban site, between the North 3rd and 4th Ring Road in Beijing (Shi et al., 2019). Although in a central location, the sampling site is surrounded by four parks containing a variety of grassed and forested areas (**Fig. 1**). The dominant plants are evergreen trees, deciduous trees, evergreen shrubs and deciduous shrubs in the urban area of Beijing (Ghirardo et al., 2016). These trees are also the main species in parks near the sampling site.

Online monitoring was conducted at the 325 m tall tower located within the grounds of the IAP tower section. For each hour, ~15 minutes were spent measuring vertical profiles of isoprene and monterpenes mixing ratios by sequentially sampling

air from the five measurement heights at 3, 15, 32, 64, and 102 m. Online measurements of ambient BVOCs were jointly conducted with colleagues from the United Kingdom who measured eddy covariance BVOC fluxes also using data from the same PTR-ToF-MS. Air samples were drawn from inlets at different heights to the ground station with high-volume pumps to minimize the residence time in the sampling lines to be less than 1 second. Then the automatic switching valves were used to achieve gradient switching. Sample air was drawn through individual 1/4 inch outer diameter (O.D.) Polytetra fluoroethylene (PTFE) sample lines at a flow rate of 3.3 L/min, with 0.3 L/min of this airflow diverted into heated (30°C) 10 L stainless steel canisters. The turnover time of air within each of the five canisters was ~ 30 min, which meant the PTR-ToF-MS could sample sequentially from each canister for just 170 sec and provide mixing ratios that were representative of the average during the previous half an hour. A further 5 minutes was spent measuring the instrument background and the remaining 40 min of each hour were for eddy covariance flux measurements. All air samples entered the PTR-ToF-MS via a 1 m long 1/4 inch O.D. PTFE line followed by a 20 cm long 1/16 inch O.D. polyetheretherketone (PEEK) inlet tube. A PTFE filter (Mitex, Merck KGaA, Ireland) was installed in front of the inlet to remove particulate matters. Trichlorobenzene was introduced into the inlet flow via diffusion through a needle valve to provide a high mass compound for mass calibration. The VOCs were measured by a PTR-ToF-MS 2000 (Ionicon Analytik GmbH, Innsbruck, Austria) housed in an air-conditioned container from November 23rd to December 12th, 2016 during the winter campaign and from June 10th to June 25th, 2017 during the summer campaign.

1.2 Instrument setup

The basic principles of PTR-ToF-MS have been described elsewhere in detail (Jordan et al., 2009; Huang et al., 2016). Briefly, the instrument consists of a hollow cathode ion source that generates a pure H_3O^+ reagent ion stream, a drift tube is used to ionize VOCs, and a high resolution time-of-flight mass spectrometer separates the ions according to their mass-to-charge ratio (*m/z*).

During the campaigns, the PTR-ToF-MS was operated under conditions of 1.9 mbar drift tube pressure, 60°C of inlet and drift temperature, and a drift tube voltage of 484 V, and *E/N* of 130 Td (where, *E* is electric field strength and *N* is the number density of a neutral gas; 1 Td is 10^{-17} V·cm^2).

Multipoint calibrations were performed twice every week using a VOC standard mixture (UK National Physical Laboratory; ~1 ± 0.10 ppmV) by dynamic dilution with two mass flow controllers (Model 8500, KOFLOC, Japan; F-201CV, Bronkhorst, Germany), which had been calibrated before use by a flowmeter (Gilian Cilibrator 2, Sensidyne, USA). Calibration curves and method detection limit (MDLs) of isoprene and α-pinene in this campaign were presented in Appendix A **Fig. S1**. The MDLs of isoprene and α-pinene were 58 and 64 pptV, respectively (Huang et al., 2017). It is worth noting that isoprene (*m/z* 69) may be overestimated due to interference from Furan and the fragmentation of 2-methyl-3-butene-2-ol (MBO) (de Gouw et al., 2003; Yuan et al., 2017). Monoterpenes (*m/z* 137) were quantified by the sensitivity of α-pinene and may be underestimated because of a small fragment in *m/z* 87 (Warneke et al., 2003).

1.3 Trace gases and meteorological data

Data of other pollutants such as carbon monoxide (CO) and O_3 were obtained from

the Beijing Air Quality Monitoring Network with online monitoring at the site Chaoyang Olympic Sports Center (39°59′01″ N, 116°23′56″ E). The meteorological data including wind direction (WD), wind speed (WS), relative humidity (RH), and temperature (*T*) were obtained from the IAP tower where these parameters were monitored at three heights (8, 120 and 240 m); solar radiation (SR) was obtained from monitored at ground level on the tower; planetary boundary layer (PBL) height was calculated online from NOAA's READY Archived Meteorology program (http://ready.arl.noaa.gov/READYamet.php).

During the winter campaign (November 23rd to December 12th, 2016), air temperature ranged from -3.8 to 11.5°C with an average of 3.4°C; relative humidity ranged 11%-92% with an average of 43%; PBL height ranged 50-2047 m with an average of 225 m; solar radiation was 70.2 W/m^2 on average with a maximum of 625.8 W/m^2. During the summer campaign (June 10th to June 25th, 2017), air temperature ranged from 17.8 to 39.9°C with an average of 27.4°C; relative humidity ranged 14%-100% with an average of 54%; PBL height ranged 50-3078 m with an average of 676 m; solar radiation was 211.4 W/m^2 on average with a maximum of 1156.0 W/m^2.

2. Results and discussion

2.1 Overview about mixing ratios of isoprene and monoterpenes

Figs. 2 and **3** showed the time series of mixing ratios of isoprene and monoterpenes as well as that of meteorological parameters (wind speed and direction, temperature, relative humidity, PBL and solar radiation) during the winter and the summer campaign, respectively.

During the winter campaign, measured mixing ratios of isoprene at the five heights ranged from 0.01 to 3.11 ppbV with averages from 0.71 ± 0.42 ppbV (102 m) to 1.41 ±

0.64 ppbV (15 m). Our measured isoprene mixing ratios (1.18 ± 0.53 ppbV) at the 3 m height was comparable with that of 1.00 ± 0.48 ppbV (**Table 1**) measured 2.5 m above ground also during November 2016 by PTR-ToF-MS at an urban site about 10 km away from the IAP tower (Sheng et al., 2018). However, measured mixing ratios of isoprene at 15 m (1.41 ± 0.64 ppbV) or at other heights in this study were much higher than those previously reported based on canister-sampling offline measurements in Beijing during the cold non-growing seasons, for example 0.22 ±0.13 ppbV observed ~15 m above ground at an urban site in Beijing during January-February 2015 (Li et al., 2019), 0.14 ± 0.14 ppbV at another urban site ~12 m above the ground in Beijing during January 2015 (Cheng et al., 2018), or even 0.04 ± 0.04 ppbV at an suburban site ~12 m above the group in Beijing during November-December, 2014 (Li et al., 2019). The mixing ratios on average were also much higher than that of 0.05 ppbV reported at a forest site 532 m above sea level in Cyprus during March 2015 (Debevec et al., 2018).

During the winter campaign, observed mixing ratios of monoterpenes ranged from below the MDL to 1.31 ppbV with similar averages at the five heights from 0.57 ± 0.20 ppbV at 3 m (the highest) to 0.42 ± 0.22 ppbV at 102 m (the lowest). The average mixing ratios of monoterpenes at 15 m was 0.54 ± 0.18 ppbV. These averages were also about an order of magnitude higher when compared to those based on canister-sampling offline measurements in Beijing, such as 0.06 ± 0.06 ppbV at an urban site ~15 m above the ground during January-February 2015 or 0.04 ± 0.04 ppbV at a suburban site ~12 m above the ground during November-December 2014 (**Table 1**; Li et al., 2019). They were also substantially much higher than that measured in situ (0.28 ± 0.31 ppbV) with

an online gas chromatography-flame ionization detector (GC-FID) system at the forest site in Cyprus during March 2015 (Debevec et al., 2018).

During the summer campaign, which captured the growing seasons of the local vegetation, observed mixing ratios of isoprene were between 0.44 and 2.51 ppbV with an average from 1.35 ± 0.51 ppbV at 102 m to 1.64 ± 0.66 ppbV at 32 m (**Table 1**). These are higher than those measured during the winter campaign. This is not surprising because isoprene is typically emitted from vegetation as a function of light and temperature (Guenther et al., 2006, 2012). They are also higher than those previously observed using offline canister-sampling measurements in Beijing during the growing seasons. For example, Xie et al. (2018) reported concentrations of 0.89 ± 0.55 ppbV at an urban site ~20 m above ground during August-September 2006, Li et al. (2019) reported concentrations of 0.93 ± 0.53 ppbV at another urban site ~8 m above ground during July-August 2014, and Gong et al. (2018) observed concentrations of 0.29 ± 0.03 ppbV at a forest site 1690 above sea level in TianJian Mountain in south China during July-August 2016 (**Table 1**).

During the summer campaign, mixing ratios of monoterpenes ranged from below detection limits to 0.62 ppbV as observed at the five heights with an average from 0.07 ± 0.06 ppbV at 102 m to 0.16 ± 0.10 ppbV at 3 m (**Table 1**). They are even lower than that of 0.28 ± 0.31 ppbV at the forest site in Cyprus during March 2015 (Debevec et al., 2018). It is worth noting that the monoterpenes concentrations at the five heights during the summer campaign were much lower than those during the winter campaign (**Table 1**). Given that biogenic monoterpene emissions are temperature and/or light dependent,

this finding is somewhat counterintuitive. This is likely the result of the combination of atmospheric chemistry and boundary layer dynamics. Evergreen trees and shrubs, which account for ~50% of Beijing's vegetation distribution (Ghirardo et al., 2016) can emit a small amount of monoterpenes, even in wintertime (Guenther et al., 2012). However, PBL height (225 m) during the winter campaign was much lower than that during the summer campaign (676 m). This would facilitate the accumulation of monoterpenes in the winter. In addition, monoterpenes have a much shorter atmospheric lifetime with respect to ozone than compared with isoprene (Seinfeld and Pandis, 1998). During the summer, the O_3 concentration (62.8 ppbV) during the summer campaign was about 7-fold that of 8.6 ppbV during the winter campaign, resulting in a much shorter chemical lifetime in the summer (Shi et al., 2019). Thus, both the strong chemical sink and the higher boundary layer contributed to the higher measured monoterpene concentrations in the summer despite stronger emission rates (Acton et al., 2018).

2.2 Vertical profiles of isoprene and monoterpenes

2.2.1 Gradient distributions

Tower-based and airborne measurements in Amazonia indicate that concentrations of BVOCs declined strongly with altitude (Kuhn et al., 2007). As showed in **Fig. 4** and **Table 1**, the highest average mixing ratios of isoprene (1.41 ± 0.61 ppbV) in the winter campaign was observed at 15 m, which is at a similar height as the tree canopy. Average mixing ratios of isoprene at 3 m was 1.18 ± 0.53 ppbV, just below that at 15 m. This was probably influenced by deposition towards the ground, as revealed in an

Amazonian rainforest when strong gradients towards the ground level from canopy height were also observed (Yanez-Serrano et al., 2015). From 15 to 102 m, isoprene mixing ratios showed a gradual decreasing trend, with the minimum of 0.71 ± 0.42 ppbV at 102 m, about 50% of that at 15 m. In the summer campaign, isoprene mixing ratio peaked at 32 m (1.64 ± 0.66 ppbV), and decreased to 15 m (1.61 ± 0.68 ppbV) and 3 m (1.49 ± 0.64 ppbV). This is probably also due to deposition towards the ground. From 32 to 102 m, it also showed a downward trend with the lowest level at 102 m (1.35 ± 0.51 ppbV), about 82% of that at 32 m. The contrast between the maximum and minimum of the averages at the five heights for isoprene was within 50% in the winter campaign but only 20% in the summer campaign, largely due to better near-surface mixing in the summer.

For monoterpenes, the highest mixing ratios were observed at 3 m during both the winter and the summer campaigns, and the average mixing ratios of monoterpenes all showed a downward trend from 3 to 102 m (**Table 1**; **Fig. 4**). During the winter campaign, the average mixing ratios of monoterpenes decrease by about 27% from 0.57 ± 0.20 ppbV at 3 m to 0.42 ± 0.22 ppbV at 102 m; whereas during the summer campaign it decrease by about 56% from 0.16 ± 0.10 to 0.07 ± 0.06 ppbV. This larger contrast in mixing ratios of monoterpenes between 3 and 102 m in the summertime reflects the influence of ozone on the scavenging of monoterpenes as discussed above.

The highest isoprene mixing ratios were observed on November 26th, 2016 in the winter campaign and June 16th, 2017 in the summer campaign. The highest mixing ratios of monoterpenes appeared were observed on November 26th, 2016 during the

288 winter campaign and on June 11th and 13th, 2017 in the summer campaign. As showed
289 in **Fig. 4**, the vertical profiles of the isoprene and monoterpenes during these days were
290 similar to that of the campaign averages, but the average mixing ratios during these
291 particular days were about 50% higher.

292 **2.2.2 Correlation of BVOCs between different heights**

293 To indicate if the mixing ratios of BVOCs at the five heights changed in a similar
294 pattern, the correlation analysis between BVOCs at the height with the highest average
295 concentration and those at other heights and were performed **(Fig. 5)**. During the winter
296 campaign, the mixing ratios of isoprene at 102, 64, 32 and 3 m were only modestly
297 correlated with those at 15 m, with correlation coefficient R^2 of 0.31-0.60. In the
298 summer, however, the mixing ratios of isoprene at other heights showed significant
299 correlations with those at 32 m with R^2 of 0.91-0.98. This is probably due to the
300 dominant contribution of local emission from plant leaves and better near-ground
301 mixing conditions in the summer. In contrary to isoprene, monoterpenes at 3 m showed
302 a much better correlation with those at other heights in the winter (R^2 = 0.54- 0.75) than
303 in the summer(R^2 = 0.78-0.95). The relatively poorer correlations of the mixing ratios
304 of monoterpenes between the different heights and the decrease in R^2 with heights,
305 might be resulted from their reaction with ozone at a much higher rate than in the winter
306 during upward transport.

307 **2.2.3 Diurnal variations at different heights**

308 As shown in **Fig. 6**, similar diurnal variations were observed at the five heights.
309 During the winter campaign, isoprene showed no obvious diurnal changes while

310 monoterpenes had the higher concentrations at night and the lowest ones occurred at
311 midday, consistent with the results by Hellen et al. (2012) and Cheng et al. (2018).
312 Unlike isoprene, monoterpenes are emitted not only directly by plants' synthesis under
313 light but also by pool storage (Oderbolz et al., 2013). For some tree species, terpenes
314 may be formed and preserved in mesophyll or glandular cells during the night and
315 evaporates as the temperature increases (Loreto and Schnitzler, 2010). Overall, the
316 diurnal variation of BVOCs is a balance between the higher emission during daytime
317 under elevated temperature or solar radiation and enhanced accumulation during
318 nighttime with lower PBL heights.

319 During the summer campaign, isoprene mixing ratios peaked at 15:00-16:00,
320 coincident with the maxima in solar radiation, and decreased from 18:00 until the
321 following morning. In the summer, the stronger emissions of BVOCs during the
322 daytime overtook the influence of changing PBL heights, thus they all had higher
323 mixing ratios during daytime than nighttime.

324 **2.3 Influencing factors and source implications**

325 As shown in Appendix A **Fig. S2**, monoterpenes were positively correlated with
326 relatively humidity (RH, $R^2 = 0.41$-0.47) during the winter campaign. Previous studies
327 demonstrated that humidity could increase monoterpenes emission rates under dry
328 conditions (Lamb et al., 1985; Schade et al., 1999). A recent study in the Mediterranean
329 also suggested that higher relative humidity and rainfall will promote the emission of
330 plant BVOCs in the dry season (Debevec et al., 2018). During the winter campaign,
331 mixing ratios of isoprene and monoterpenes were both elevated on November 25th and

December 3rd-4th, largely due to their accumulation in a shallow boundary layer heights and lower wind speeds **(Fig. 2)**; the higher relative humidity might also be a contributing factor to elevated mixing ratios during these two episodes. Except humidity, no further significant correlations between isoprene and monoterpeens and other meteorological parameters during the winter campaign.

The mixing ratios of isoprene were significantly correlated with temperature (R^2 = 0.73-0.86) but negatively correlated with relative humidity (R^2 = 0.22-0.39). In the summer campaign, isoprene mixing ratios were the highest on June 14th-17th and 20th-21st when the temperature and solar radiation were higher **(Fig. 3)**. Although biogenic emissions of isoprene are known to be both light and temperature dependent (Guenther et al., 2006), no correlation between isoprene and light were observed during either measurement campaign. No significant correlations between the monoterpenes and meteorological parameters were found in the summer.

To further examine if there were sources of BVOCs other than emission from plant leaves, the relationship between BVOCs and other traces gases were also investigated. Monoterpenes showed significant correlations with CO and acetonitrile in the winter as observed at the 3 m height with R^2 of 0.54 and 0.71, respectively **(Fig. 7)**. Since CO is a typical tracer of incomplete combustion of biomass or fossil fuels (Parrish et al., 2009; Zhang et al., 2015) and acetonitrile was a marker of biomass burning (Fang et al., 2017), this good correlation between monoterpenes and combustion tracers at 3 m near the ground suggests that combustion sources, particularly biomass burning, might have contributed to monoterpenes at the IAP site. Indeed, biomass burning has been reported

as an anthropogenic source of monoterpenes (Andreae and Merlet, 2001; Stockwell et al., 2015). In addition, wintertime heating in Beijing started on November 15th, and coal consumption and residential biomass were still the main fuels for central heating in Beijing (Beijing Municipal Bureau of Statistics, 2017; Yang et al., 2018). Thus, it was possible that combustion processes contributed to the emission of monoterpenes in the winter. Isoprene did not show a significant correlation with combustion tracers.

3. Conclusions

The mixing ratios of isoprene and total monoterpenes mixing ratios were measured online with a PTR-ToF-MS at five heights in central Beijing during two contrasting seasons (winter 2016 and summer 2017). Observed mixing ratios of isoprene and monoterpenes based on online measurements at the five heights were much higher than those previous measured by offline canister measurements. At the lowest height of 3 m, the average mixing ratios of isoprene reached 1.49 ± 0.64 ppbV in the summer and 1.18 ± 0.53 ppbV in the winter, suggesting potential important contribution to ozone formation by BVOCs even in the urban areas of Beijing.

Among the five heights, average mixing ratios of isoprene were highest at 32 m (1.64 ± 0.66 ppbV) in the summer and 15 m (1.41 ± 0.64 ppbV) in the winter. From the height with the highest average isoprene mixing ratios, isoprene showed a downward trend towards the ground and towards the height of 102 m. Mixing ratios of monoterpenes were highest at 3 m both in the winter (0.71 ± 0.42 ppbV) and the summer (0.16 ± 0.10 ppbV), and they decreased with altitude during both the winter and summer campaigns. The main reason for the lower ambient mixing ratios of monoterpenes

observed in the summer, when higher emissions occur, is much higher levels of O_3 and reduced the atmospheric lifetime of the monoterpenes.

At the five heights, isoprene observed in summer and monoterpenes observed in winter, showed highly significant mutual correlations, while isoprene observed in winter or monoterpenes observed in the summer showed poorer mutual correlations, largely due to different roles play by emissions, atmospheric oxidation and dispersion conditions in the two seasons. Isoprene showed significant correlations with temperature in the summer while monoterpenes with relative humidity in the winter. In addition, in winter monoterpenes showed significantly positive correlations with CO and acetonitrile, suggesting possible emissions from anthropogenic sources, particularly combustion sources such as biomass burning and coal combustion.

Acknowledgments

This study was supported by the National Natural Science Foundation of China (Nos. 41571130031, 41673116, 41703112, 41603070), the Natural Environment Research Council (Nos. NE/N006992/1 and NE/N006976/1), Theme-based Research Scheme (No. T24-504/17-N), Youth Innovation Promotion Association of the Chinese Academy of Sciences (No. 2017406) and Natural Science Foundation of Guangdong Province (No. 2016A030310117). ZS acknowledges financial support from Natural Environment Research Council (NE/N007190/1). We acknowledge the support from Pingqing Fu, Zifa Wang, Jie Li and Yele Sun from IAP for hosting the Atmospheric Pollution and Human Health in a Developing Megacity (APHH-Beijing) campaign at IAP. We thank Zongbo Shi, Di Liu, Roy Harrison, Tuan Vu and Bill Bloss from the University of

Birmingham, Siyao Yue, Liangfang Wei, Hong Ren, Qiaorong Xie, Wanyu Zhao, Linjie Li, Ping Li, Shengjie Hou, Qingqing Wang from IAP, Rachel Dunmore, Ally Lewis and James Lee from the University of York, Kebin He and Xiaoting Cheng from Tsinghua University, and James Allan and Hugh Coe from the University of Manchester for providing logistic and scientific support for the field campaigns.

Appendix A. Supplementary data

Supplementary data associated with this article can be found in the online version at xxxxxx.

References

Acton, W.J.F., Jud, W., Ghirardo, A., Wohlfahrt, G., Hewitt, C.N., Taylor, J.E., et al. 2018. The effect of ozone fumigation on the biogenic volatile organic compounds (BVOCs) emitted from Brassica napus above- and below-ground. PLoS ONE 13(12), e0208825.

Ahn, J.H., Deep, A., Kim, K.H., 2016. The storage stability of biogenic volatile organic compounds (BVOCs) in polyester aluminum bags. Atmos. Environ. 141, 430-434.

Andreae, M.O., Merlet, P., 2001. Emission of trace gases and aerosols from biomass burning, Global Biogeochem. Cy., 15, 955–966.

Arnts, R.R., 2008. Reduction of biogenic VOC sampling losses from ozone via trans-2-Butene addition. Environ. Sci. Technol. 42 (20), 7663-7669.

Atkinson, R., 2000. Atmospheric chemistry of VOCs and NOx. Atmos. Environ. 34 (12-14), 2063-2101.

Bai, J.H., Guenther, A., Turnipseed, A., Duhl, T., Greenberg, J., 2017. Seasonal and interannual variations in whole-ecosystem BVOC emissions from a subtropical plantation in China. Atmos. Environ. 161, 176-190.

Baker, B., Bai, J.H., Johnson, C., Cai, Z.T., Li, Q.J., Wang, Y.F., et al., 2005. Wet and dry season ecosystem level fluxes of isoprene and monoterpenes from a southeast

425 Asian secondary forest and rubber tree plantation. Atmos. Environ. 39 (2), 381-
426 390.
427 Beijing Municipal Bureau of Statistics (BMBS): Bejing Statistical Yearbook 2017,
428 China Statistics Press, Beijing, 2017.
429 Cheng, X., Li, H., Zhang, Y.J., Li, Y.P., Zhang, W.Q., Wang, X.Z, et al., 2018.
430 Atmospheric isoprene and monoterpenes in a typical urban area of Beijing:
431 Pollution characterization, chemical reactivity and source identification. J.
432 Environ. Sci. 71, 150-167.
433 Curci, G., Beekmann, M., Vautard, R., Smiatek, G., Steinbrecher, R., Theloke, J., et al.,
434 2009. Modelling study of the impact of isoprene and terpene biogenic emissions
435 on European ozone levels. Atmos. Environ. 43 (7), 1444-1455.
436 de Gouw, J., Warneke, C., 2007. Measurements of volatile organic compounds in the
437 earth's atmosphere using proton-transfer-reaction mass spectrometry. Mass
438 Spectrom. Rev. 26 (2), 223-257.
439 de Gouw, J.A., Goldan, P.D., Warneke, C., Kuster, W.C., Roberts, J.M., Marchewka,
440 M., et al., 2003. Validation of proton transfer reaction-mass spectrometry (PTR-
441 MS) measurements of gas-phase organic compounds in the atmosphere during the
442 New England Air Quality Study (NEAQS) in 2002. J. Geophys. Res. 108 (D21).
443 Debevec, C., Sauvage, S., Gros, V., Sellegri, K., Sciare, J., Pikridas, M., et al., 2018.
444 Driving parameters of biogenic volatile organic compounds and consequences on
445 new particle formation observed at an eastern Mediterranean background site.
446 Atmos. Chem. Phys. 18 (19), 14297-14325.
447 Ding, X., Wang, X.M., Gao, B., Fu, X.X., He, Q.F., Zhao, X.Y., et al., 2012. Tracer-
448 based estimation of secondary organic carbon in the Pearl River Delta, south China.
449 J. Geophys. Res. 117, D05313.
450 Duan, J.C., Tan, J.H., Yang, L., Wu, S., Hao, J.M., 2008. Concentration, sources and
451 ozone formation potential of volatile organic compounds (VOCs) during ozone
452 episode in Beijing. Atmos. Res. 88 (1), 25-35.
453 Eerdekens, G., Ganzeveld, L., de Arellano, J.V.-G., Kluepfel, T., Sinha, V., Yassaa, N.,
454 et al., 2009. Flux estimates of isoprene, methanol and acetone from airborne PTR-

455 MS measurements over the tropical rainforest during the GABRIEL 2005
456 campaign. Atmos. Chem. Phys. 9 (13), 4207-4227.
457 Fang, Z., Deng, W., Zhang, Y.L., Ding, X., Tang, M.J., Liu, T.Y., et al., 2017. Open
458 burning of rice, corn and wheat straws: primary emissions, photochemical aging,
459 and secondary organic aerosol formation. Atmos. Chem. Phys. 17 (24), 14821-
460 14839.
461 Fick, J., Pommer, L., Andersson, B., Nilsson, C., 2001. Ozone removal in the sampling
462 of parts per billion levels of terpenoid compounds: An evaluation of different
463 scrubber materials. Environ. Sci. Technol. 35 (7), 1458-1462.
464 Fu, P., Kawamura, K., Chen, J., Barrie, L.A., 2009. Isoprene, Monoterpene, and
465 Sesquiterpene oxidation products in the high Arctic aerosols during late Winter to
466 early Summer. Environ. Sci. Technol. 43 (11), 4022-4028.
467 Ghirardo, A., Xie, J., Zheng, X., Wang, Y., Grote, R., Block, K., et al., 2016. Urban
468 stress-induced biogenic VOC emissions and SOA-forming potentials in Beijing.
469 Atmos. Chem. Phys. 16 (5), 2901-2920.
470 Gong, D.C., Wang, H., Zhang, S.Y., Wang, Y., Liu, S.C., Guo, H., et al., 2018. Low-
471 level summertime isoprene observed at a forested mountaintop site in southern
472 China: implications for strong regional atmospheric oxidative capacity. Atmos.
473 Chem. Phys. 18 (19), 14417-14432.
474 Greenberg, J.P., Guenther, A., Zimmerman, P., Baugh, W., Geron, C., Davis, K., et al.,
475 1999. Tethered balloon measurements of biogenic VOCs in the atmospheric
476 boundary layer. Atmos. Environ. 33 (6), 855-867.
477 Guenther, A.B., Karl, T., Harley, P., Wiedinmyer, C., Palmer, P. I., Geron, C., 2006.
478 Estimates of global terrestrial isoprene emissions using MEGAN (Model of
479 Emissions of Gases and Aerosols from Nature), Atmos. Chem. Phys., 6, 3181-
480 3210.
481 Guenther, A.B., Jiang, X., Heald, C.L., Sakulyanontvittaya, T., Duhl, T., Emmons, L.K.,
482 et al., 2012. The model of emissions of gases and aerosols from nature version 2.1
483 (MEGAN2.1): An extended and updated framework for modeling biogenic
484 emissions. Geosci. Model Dev. 5 (6), 1471-1492.

485 Hallquist, M., Wenger, J.C., Baltensperger, U., Rudich, Y., Simpson, D., Claeys, M., et
486 al., 2009. The formation, properties and impact of secondary organic aerosol:
487 current and emerging issues. Atmos. Chem. Phys. 9 (14), 5155-5236.
488 He, H., Li, C., Loughner, C.P., Li, Z.Q., Krotkov, N.A., Yang, K., et al., 2012. SO_2 over
489 central China: Measurements, numerical simulations and the tropospheric sulfur
490 budget. J. Geophys. Res. 117, D00K37.
491 Hellen, H., Tykka, T., Hakola, H., 2012. Importance of monoterpenes and isoprene in
492 urban air in northern Europe. Atmos. Environ. 59, 59-66.
493 Helmig, D., Balsley, B., Davis, K., Kuck, L.R., Jensen, M., Bognar, J., et al., 1998.
494 Vertical profiling and determination of landscape fluxes of biogenic nonmethane
495 hydrocarbons within the planetary boundary layer in the Peruvian Amazon. J.
496 Geophys. Res. 103 (D19), 25519-25532.
497 Henze, D.K., Seinfeld, J.H., 2006. Global secondary organic aerosol from isoprene
498 oxidation. Geophys. Res. Lett. 33 (9).
499 Hollaway, M., Wild, O., Yang, T., Sun, Y., Xu, W., Xie, C., et al., 2019. Photochemical
500 impacts of haze pollution in an urban environment. Atmos. Chem. Phys. 2019 (19)
501 9699-9714.
502 Huang, Z.H., Zhang, Y.L., Yan, Q., Zhang, Z., Wang, X.M., 2016. Real-time monitoring
503 of respiratory absorption factors of volatile organic compounds in ambient air by
504 proton transfer reaction time-of-flight mass spectrometry. J. Hazard. Mater. 320,
505 547-555.
506 Huang, Z.H., Zhang, Y.L., Yan, Q., Wang, Z.Y., Zhang, Z., Wang, X.M., 2017.
507 Decreased human respiratory absorption factors of aromatic hydrocarbons at
508 lower exposure levels: The dual effect in reducing ambient air toxics. Environ. Sci.
509 Technol. Lett. 4 (11), 463-469.
510 Jo, W.K., Kim, K.Y., 2002. Vertical variability of volatile organic compound (VOC)
511 levels in ambient air of high-rise apartment buildings with and without occurrence
512 of surface inversion. Atmos. Environ. 36, 5645-5652.
513 Jordan, A., Haidacher, S., Hanel, G., Hartungen, E., Maerk, L., Seehauser, H., et al.,
514 2009. A high resolution and high sensitivity proton-transfer-reaction time-of-flight

515 mass spectrometer (PTR-TOF-MS). Int. J. Mass spectrom. 286, 122-128.
516 Kesselmeier, J., Kuhn, U., Rottenberger, S., Biesenthal, T., Wolf, A., Schebeske, G., et
517 al., 2002. Concentrations and species composition of atmospheric volatile organic
518 compounds (VOCs) as observed during the wet and dry season in Rondonia
519 (Amazonia). J. Geophys. Res. 107 (D20), 8053.
520 Kuhn, U., Andreae, M.O., Ammann, C., Araujo, A.C., Brancaleoni, E., Ciccioli, P., et
521 al., 2007. Isoprene and monoterpene fluxes from Central Amazonian rainforest
522 inferred from tower-based and airborne measurements, and implications on the
523 atmospheric chemistry and the local carbon budget. Atmos. Chem. Phys. 7 (11),
524 2855-2879.
525 Lamb, B., Westberg, H., Allwine, G., Quarles, T., 1985. Biogenic hydrocarbon
526 emissions from deciduous and coniferous trees in United-States. J. Geophys. Res.
527 90 (ND1), 2380-2390.
528 Li, K., Li, J.L., Tong, S.R., Wang, W.G., Huang, R.J., Ge, M.F., 2019. Characteristics
529 of wintertime VOCs in suburban and urban Beijing: concentrations, emission
530 ratios, and festival effects. Atmos. Chem. Phys. 19 (12), 8021-8036.
531 Lin, Y.H., Zhang, H., Pye, H.O.T., Zhang, Z., Marth, W.J., Park, S., et al., 2013. Epoxide
532 as a precursor to secondary organic aerosol formation from isoprene
533 photooxidation in the presence of nitrogen oxides. Proc. Natl. Acad. Sci. USA 110
534 (17), 6718-6723.
535 Liu, C.T., Ma, Z.B., Mu, Y.J., Liu, J.F., Zhang, C.L., Zhang, Y.Y., et al., 2017. The levels,
536 variation characteristics, and sources of atmospheric non-methane hydrocarbon
537 compounds during wintertime in Beijing, China. Atmos. Chem. Phys. 17 (17),
538 10633-10649.
539 Liu, C.T., Mu, Y.J., Zhang, C.L., Zhang, Z.B., Zhang, Y.Y., Liu, J.F., et al., 2016.
540 Development of gas chromatography-flame ionization detection system with a
541 single column and liquid nitrogen-free for measuring atmospheric C2-C12
542 hydrocarbons. J. Chromatogr. A 1427, 134-141.
543 Loreto, F., Schnitzler, J.-P., 2010. Abiotic stresses and induced BVOCs. Trends Plant
544 Sci. 15 (3), 154-166.

Martinsson, J., Monteil, G., Sporre, M.K., Hansen, A.M.K., Kristensson, A., Stenstrom, K.E., et al., 2017. Exploring sources of biogenic secondary organic aerosol compounds using chemical analysis and the FLEXPART model. Atmos. Chem. Phys. 17 (18), 11025-11040.

Mo, Z.W., Shao, M., Wang, W.J., Liu, Y., Wang, M., Lu, S.H., 2018. Evaluation of biogenic isoprene emissions and their contribution to ozone formation by ground-based measurements in Beijing, China. Sci. Total Environ. 627, 1485-1494.

Oderbolz, D.C., Aksoyoglu, S., Keller, J., Barmpadimos, I., Steinbrecher, R., Skjoth, C.A., et al., 2013. A comprehensive emission inventory of biogenic volatile organic compounds in Europe: Improved seasonality and land-cover. Atmos. Chem. Phys. 13 (4), 1689-1712.

Parrish, D.D., Kuster, W.C., Shao, M., Yokouchi, Y., Kondo, Y., Goldan, P.D., et al., 2009. Comparison of air pollutant emissions among mega-cities. Atmos. Environ. 43 (40), 6435-6441.

Reeves, C.E., Formenti, P., Afif, C., Ancellet, G., Attie, J.L., Bechara, J., et al., 2010. Chemical and aerosol characterisation of the troposphere over West Africa during the monsoon period as part of AMMA. Atmos. Chem. Phys. 10 (16), 7575-7601.

Ryerson, T.B., Trainer, M., Holloway, J.S., Parrish, D.D., Huey, L.G., Sueper, D.T., et al., 2001. Observations of ozone formation in power plant plumes and implications for ozone control strategies. Science, 292 (5517), 719-723.

Schade, G.W., Goldstein, A.H., Lamanna, M.S., 1999. Are monoterpene emissions influenced by humidity? Geophys. Res. Lett. 26 (14), 2187-2190.

Seinfeld, J.H., Pandis, S.N., 1998. Atmospheric Chemistry and Physics: From Air Pollution to Climate Changes. Wiley, New York, USA.

Sheng, J.J., Zhao, D.L., Ding, D.P., Li, X., Huang, M.Y., Gao, Y., et al., 2018. Characterizing the level, photochemical reactivity, emission, and source contribution of the volatile organic compounds based on PTR-TOF-MS during winter haze period in Beijing, China. Atmos. Res. 212, 54-63.

Shi, Z.B., Vu, T., Kotthaus, S., Harrison, R.M., Grimmond, S., Yue, S.Y., et al., 2019. Introduction to the special issue "In-depth study of air pollution sources and

processes within Beijing and its surrounding region (APHH-Beijing)". Atmos. Chem. Phys. 19 (11), 7519-7546.

Shilling, J.E., Zaveri, R.A., Fast, J.D., Kleinman, L., Alexander, M.L., Canagaratna, M.R., et al., 2013. Enhanced SOA formation from mixed anthropogenic and biogenic emissions during the CARES campaign. Atmos. Chem. Phys. 13 (4), 2091-2113.

Stockwell, C.E., Veres, P.R., Williams, J., Yokelson, R.J., 2015. Characterization of biomass burning emissions from cooking fires, peat, crop residue, and other fuels with high-resolution proton-transfer-reaction time-of-flight mass spectrometry. Atmos. Chem. Phys. 15 (2), 845-865.

Sun, J., Wang, Y.S., Wu, F.K., Tang, G.Q., Wang, L.L., Wang, Y.H., et al., 2018. Vertical characteristics of VOCs in the lower troposphere over the North China Plain during pollution periods. Environ. Pollut. 236, 907-915.

Warneke, C., De Gouw, J.A., Kuster, W.C., Goldan, P.D., Fall, R., 2003. Validation of atmospheric VOC measurements by proton-transfer-reaction mass spectrometry using a gas-chromatographic pre-separation method. Environ. Sci. Technol. 37 (11), 2494-2501.

Xie, X., Shao, M., Liu, Y., Lu, S.H., Chang, C.-C., Chen, Z.-M., 2008. Estimate of initial isoprene contribution to ozone formation potential in Beijing, China. Atmos. Environ. 42 (24), 6000-6010.

Xu, L., Guo, H.Y., Boyd, C.M., Klein, M., Bougiatioti, A., Cerully, K.M., et al., 2015. Effects of anthropogenic emissions on aerosol formation from isoprene and monoterpenes in the southeastern United States. Proc. Natl. Acad. Sci. USA. 112 (1), 37-42.

Yanez-Serrano, A.M., Noelscher, A.C., Williams, J., Wolff, S., Alves, E., Martins, G.A., et al., 2015. Diel and seasonal changes of biogenic volatile organic compounds within and above an Amazonian rainforest. Atmos. Chem. Phys. 15 (6), 3359-3378.

Yang, W.Q., Zhang, Y.L., Wang, X.M., Li, S., Zhu, M., Yu, Q.Q., et al., 2018. Volatile organic compounds at a rural site in Beijing: influence of temporary emission control and wintertime heating. Atmos. Chem. Phys. 18 (17), 12663-12682.

Yuan, B., Koss, A.R., Warneke, C., Coggon, M., Sekimoto, K., de Gouw, J.A., 2017. Proton-Transfer-Reaction Mass Spectrometry: Applications in atmospheric sciences. Chem. Rev. 117 (21), 13187-13229.

Zhang, H.F., Yee, L.D., Lee, B.H., Curtis, M.P., Worton, D.R., Isaacman-VanWertz, G., et al., 2018. Monoterpenes are the largest source of summertime organic aerosol in the southeastern United States. Proc. Natl. Acad. Sci. USA 115 (9), 2038-2043.

Zhang, Z., Zhang, Y.L., Wang, X.M., Lu, S.J., Huang, Z.H., Huang, X.Y., et al., 2016. Spatiotemporal patterns and source implications of aromatic hydrocarbons at six rural sites across China's developed coastal regions. J. Geophys. Res. 121 (11), 6669-6687.

Table 1 Comparison of average mixing ratios of isoprene and monoterpenes (average ± standard deviation) observed at IAP tower in our study with those reported in Beijing and other forest sites.

Sampling site	Height (m)	Type	Isoprene (ppbV)	Monoterpenes (ppbV)	Study periods
PKU, Beijing[a]	~20	Urban	0.89 ± 0.55	NA	Aug.-Sep., 2006
NCNST, Beijing[b]	~15	Urban	0.22 ± 0.13	0.06 ± 0.06	Jan.-Feb., 2015
YUFA, Beijing[b]	~12	Rural	0.64 ± 0.44	NA	Jan.-Feb., 2015
UCAS, Beijing[b]	~12	Suburban	0.04 ± 0.04	0.04 ± 0.04	Nov.-Dec., 2014
CRAES, Beijing[c]	8	Urban	0.93 ± 0.53	NA	Jul.-Aug., 2014
			0.14 ± 0.14	NA	Jan., 2015
BAAF, Beijing[d]	2.5	Urban	1.00 ± 0.48	NA	Dec., 2016
Cyprus[e]	532[h]	Forest	0.05 ± 0.01	0.28 ± 0.31	Mar., 2015
Mt. TianJing, China[f]	1690[h]	Forest	0.29 ± 0.03	NA	Jul.-Aug., 2016
IAP, Beijing[g]	3	Urban	1.18 ± 0.53	0.57 ± 0.20	Nov.-Dec., 2016
	15		1.41 ± 0.64	0.54 ± 0.18	
	32		0.99 ± 0.44	0.52 ± 0.17	
	64		0.83 ± 0.43	0.49 ± 0.17	
	102		0.71 ± 0.42	0.42 ± 0.22	
IAP, Beijing[g]	3	Urban	1.49 ± 0.64	0.16 ± 0.10	Jun., 2017
	15		1.61 ± 0.68	0.14 ± 0.09	
	32		1.64 ± 0.66	0.11 ± 0.08	
	64		1.37 ± 0.62	0.09 ± 0.07	
	102		1.35 ± 0.51	0.07 ± 0.06	

[a]Xie et al., 2008, [b]Li et al., 2019, [c]Cheng et al., 2018, [d]Sheng et al., 2018, [e]Debevec et al., 2018, [f]Gong et al., 2018, [g]This study; [h]Meters above sea level. NA: not available; PKU: Peking University; NCNST: the National Center for Nanoscience and Technology of China; YUFA: Yu Fa Town; UCAS: the University of Chinese Academy of Sciences; CRAES: the Chinese Research Academy of Environmental Sciences; BAAF: the Beijing Academy of Agriculture and Forestry; Mt. TianJing: TianJing Mountain.

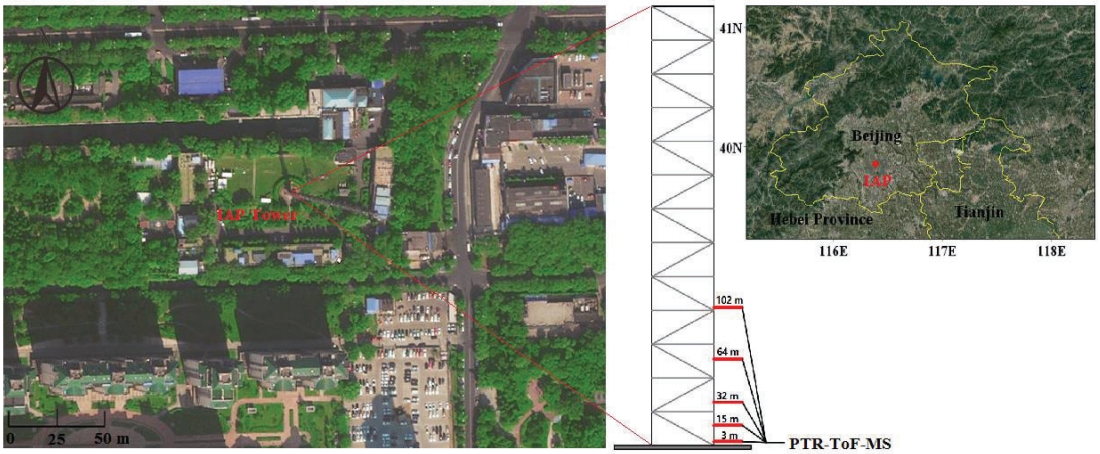

625

626 **Fig. 1** A map showing the surroundings of the Institute of Atmospheric Physics (IAP)
627 tower (left), a diagram showing the sampling heights in the IAP tower (middle) and the
628 location of IAP tower in Beijing (upper-right corner).

629

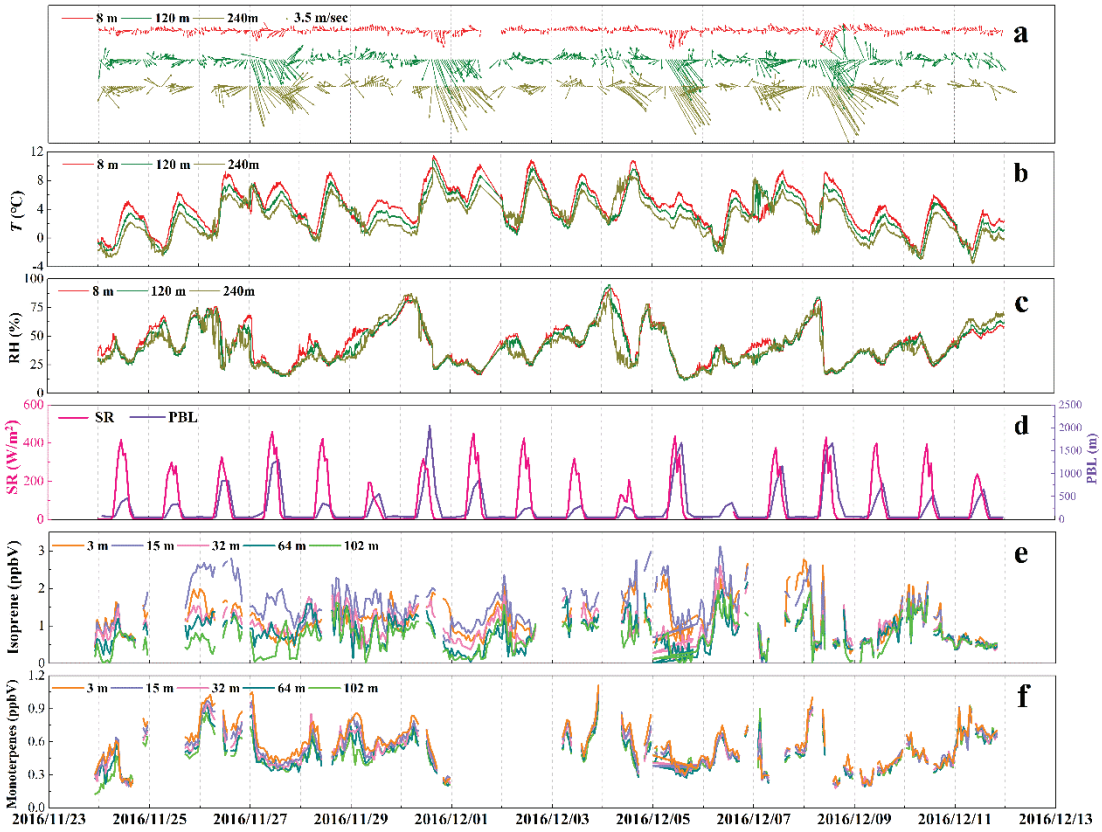

630

631 **Fig. 2** Time series of (a) wind speed and wind direction, (b) temperature (*T*), (c) relative

632 humidity (RH), (d) solar radiation (SR) and planetary boundary layer height (PBL), (e)

633 mixing ratios of isoprene and (f) monoterpenes during the winter campaign in 2016.

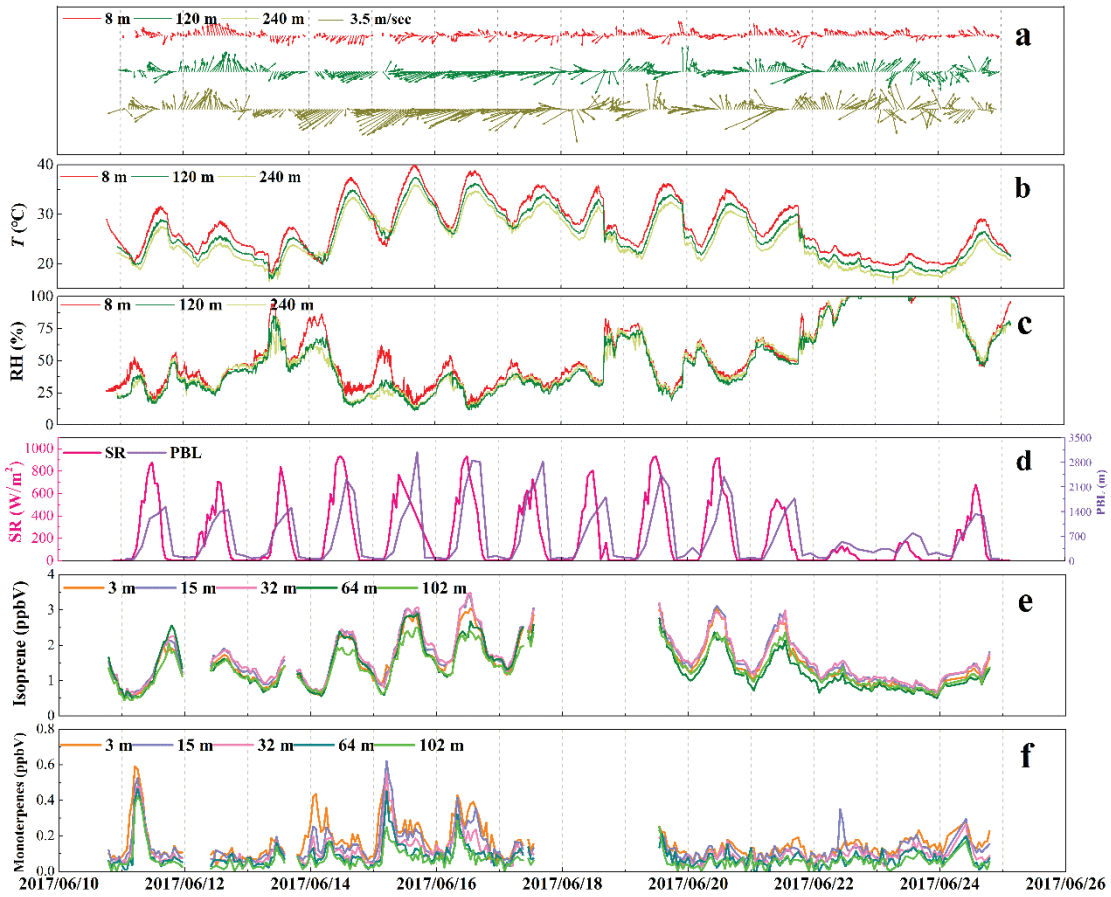

634

635 **Fig. 3** Time series of (a) wind speed and wind direction, (b) temperature (*T*), (c) relative

636 humidity (RH), (d) solar radiation (SR) and planetary boundary layer height (PBL), (e)

637 mixing ratios of isoprene and (f) monoterpenes during the summer campaign in 2017.

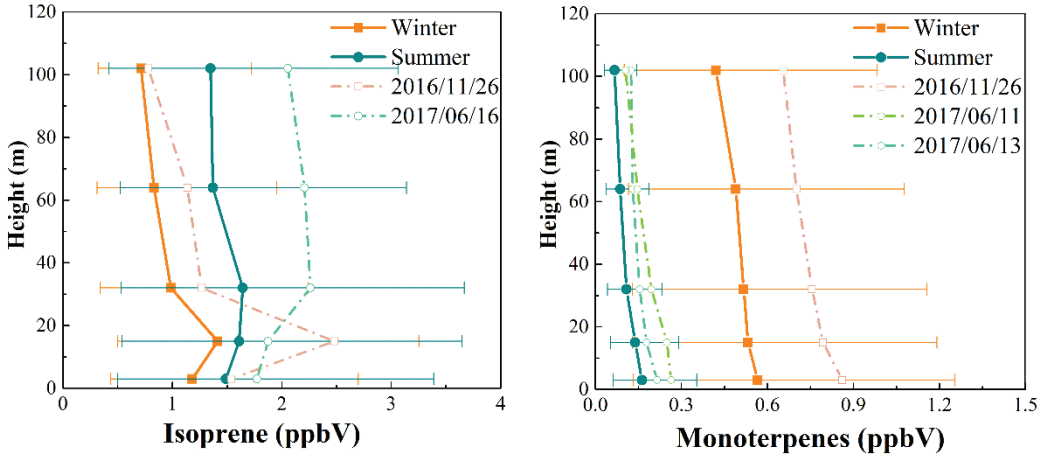

638

639 **Fig. 4** Vertical profiles for mixing ratios of isoprene and monoterpenes during the
640 winter and the summer campaigns. Range bars represent the 25% and 75% percentiles.
641 Solid lines repesents the averages during the whole summer or winter campaign; dashed
642 lines are the days (2016/11/26, 2017/06/11, 2017/06/13 and 2017/06/16) when higher
643 levels of isoprene or monoterpenes occurred.

644

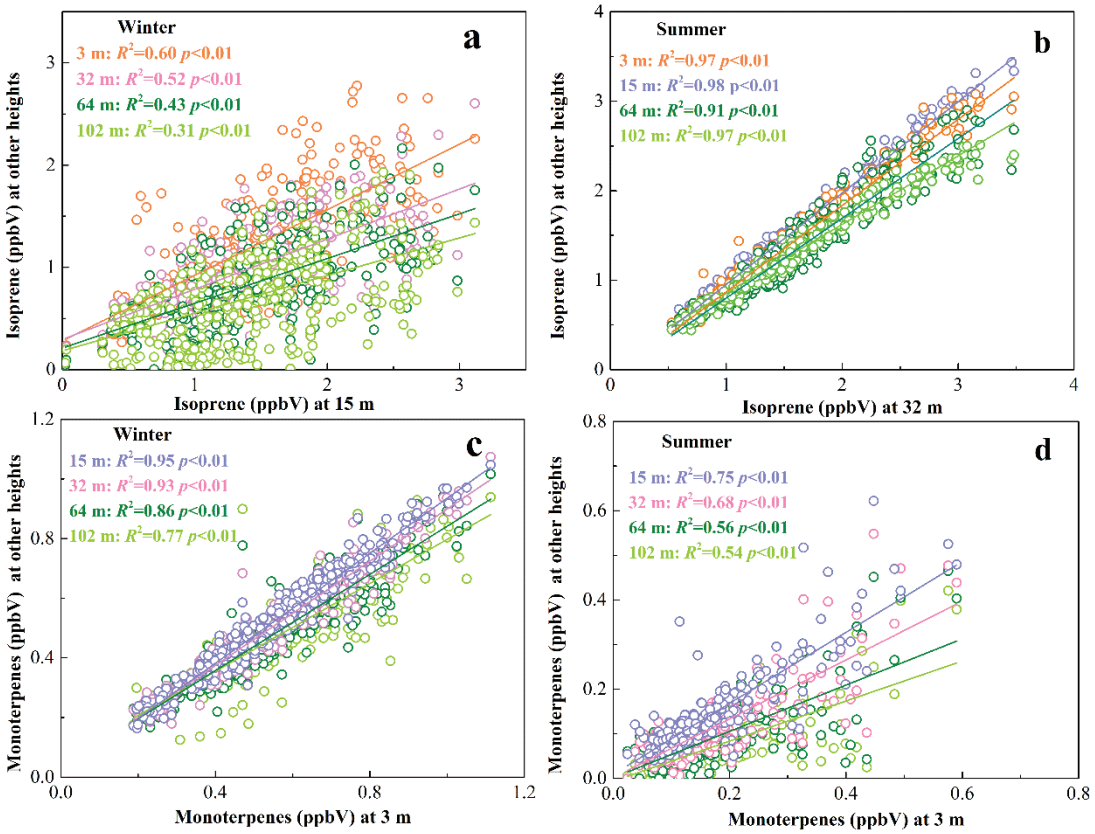

645

646 **Fig. 5** (a) Correlations between the isoprene concentrations at 15 m and those at other
647 heights in the winter; (b) correlations between the isoprene mixing ratios at 32 m and
648 those at other heights in the summer; correlations between the mixing ratios of
649 monoterpenes at 3 m and those at other heights (c) in the winter and (d) in the summer.

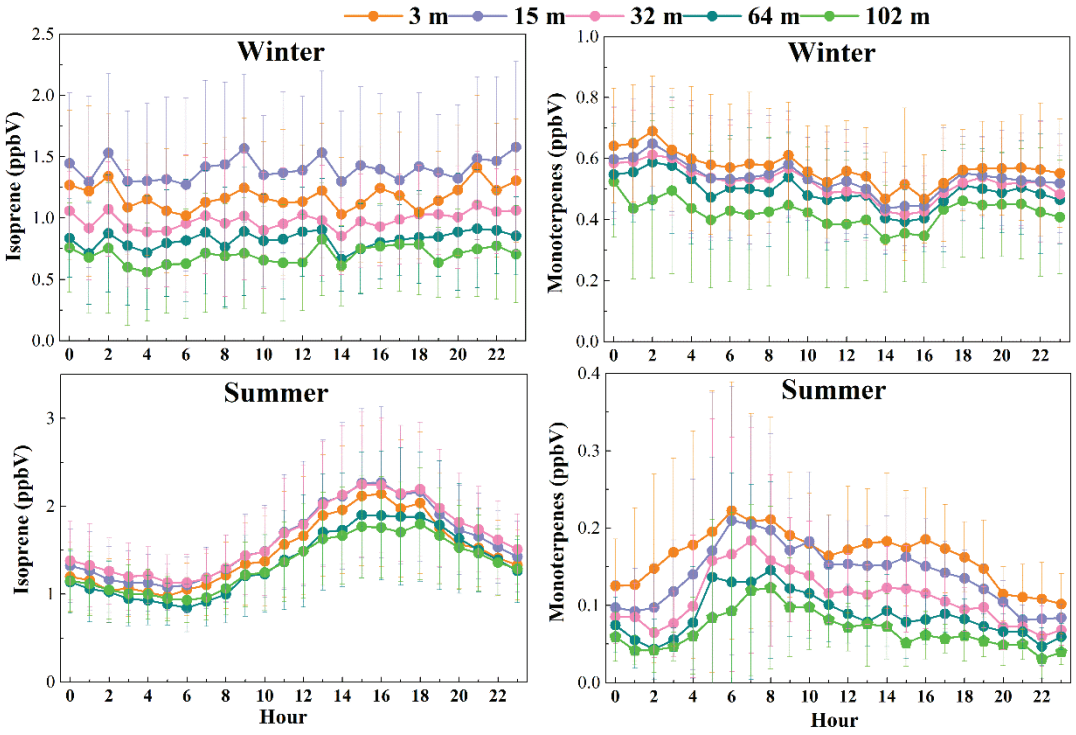

650

651 **Fig. 6** Diurnal variations of isoprene and monoterpenes observed at the five heights in
652 the winter 2016 campaign and the summer 2017 campaign. Range bars are expressed
653 the 25% and 75% percentiles.

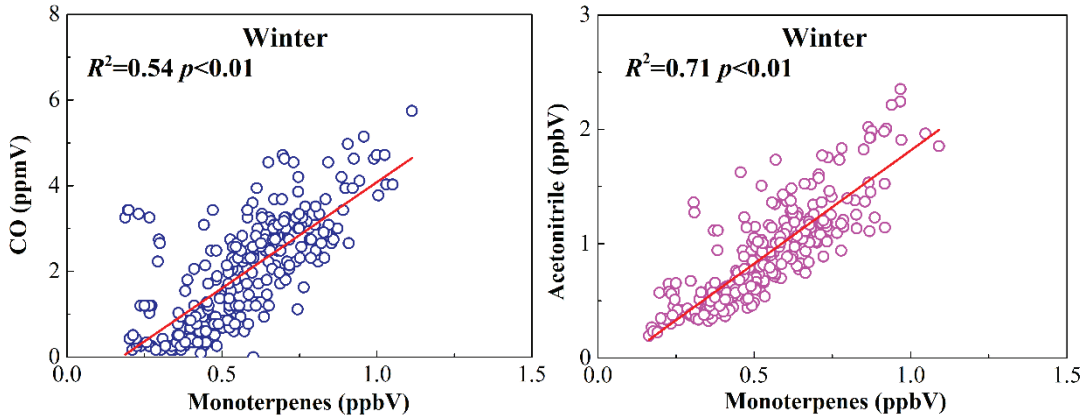

654

655 **Fig. 7** Correlations of monoterpenes with CO and acetonitrile at 3 m during the 2016

656 winter campaign.